

Ricci-Notation Tensor Framework for Model-Based Approaches to Imaging

Dileepan Joseph (dil.joseph@ualberta.ca)

Department of Electrical and Computer Engineering
University of Alberta, Edmonton, AB, Canada

December 8, 2023

Abstract

Model-based approaches to imaging, like specialized image enhancements in astronomy, favour physics-based models which facilitate explanations of relationships between observed inputs and computed outputs. While this paper features a tutorial example, inspired by exoplanet imaging, that reveals embedded 2D fast Fourier transforms in an image enhancement model, the work is actually about the tensor algebra and software, or tensor frameworks, available for model-based imaging. The paper proposes a Ricci-notation tensor (RT) framework, comprising an extended Ricci notation, which aligns well with the symbolic dual-index algebra of non-Euclidean geometry, and codesigned object-oriented software, called the RTToolbox for MATLAB. Extensions offer novel representations for entrywise, pagewise, and broadcasting operations popular in extended matrix-vector (EMV) frameworks for imaging. Complementing the EMV algebra computable with MATLAB, the RTToolbox demonstrates programmatic and computational efficiency thanks to careful design of tensor and dual-index classes. Compared to a numeric tensor predecessor, the RT framework enables superior ways to model imaging problems and, thereby, to develop solutions.

I. INTRODUCTION

“Tensors” easily associate with learning-based approaches to imaging. After all, TensorFlow from Google Brain [1] and Tensor Comprehensions from Facebook AI [2] are machine learning systems connected with a well known deep learning revolution in object detection and classification. Nonetheless, imaging researchers like Mai *et al.* [3] highlight the importance of model-based tensor approaches, emphasizing explanatory value. Mai *et al.* also argue that a model-based approach helps to reduce the training data requirements for a learning-based approach, yielding what is in effect a hybrid approach.

Imaging researchers are finding advantages of model-based tensor approaches in a variety of applications. These include: multi-exposure, multi-focus, and hyper/multi-spectral image fusion to increase dynamic range, depth-of-field, and spatial resolution [3], [4], [5]; inpainting, or tensor completion, of missing or corrupt pixels in images and videos, even rows or columns of the same [6], [7]; deblurring, or image restoration, posed as a constrained inverse problem often with added noise [8], [9], [10]; compressive sensing, a mixture of computational imaging and image compression, for light field imaging (LFI), synthetic aperture radar, and hyperspectral imaging modalities [11], [12], [13]; other constrained image enhancements, like ones that enforce 3D spherical invariances [14]; and image quality assessments, like ones tailored for LFI [15].

Model-based imaging research involving tensors [3]–[15] exhibits patterns. Papers typically have a section or subsection, on fundamentals, that addresses unary, binary, and N -ary operations expressible with tensors, like multi-way or multi-index contractions, Kronecker and Khatri-Rao products, and Tucker, canonical polyadic (CP), and tensor trains (TT) constructs. More fundamental than operations, authors discuss an n -mode notation, especially for decomposition constructs, an index notation, also called Einstein notation, or a hybrid notation thereof. Sometimes, extended matrix-vector (EMV) operators are employed to represent Hadamard, or entrywise, and Kronecker, or outer, products. Notation can resemble MATLAB or Python+NumPy syntax for multidimensional arrays (MDAs). Instead of matrix-vector (MV) or EMV algebra, authors prefer tensor algebra to represent and manipulate high-order image relationships, including generalizations of the singular value decomposition (SVD) for rank reduction and feature extraction, akin to principal components analysis, and optimizations where images are the unknown variables in a functional that suffers upon vectorization of variables.

Whereas tensor notations and operations are in some senses implementation agnostic, a brief survey of tensor software is in order. Because its components, like the Cyclops Tensor Framework (CTF) [16], [17], may apply to tensor contractions, completions, and decompositions for imaging, the NorthWest Chemistry (NWChem) software ecosystem is noteworthy [18], [19]. With the Tensor Contraction Engine (TCE) and the Tensor Algebra for Many-Body Methods (TAMM) [20], [21], this ecosystem targets massively parallel computing and large-scale molecular simulations. Intended more for imaging and for desktop parallel computing, Tensor Learning in Python (TensorLy) offers tensor decompositions to improve efficiency, robustness, and explainability of deep learning networks [22], [23]. For desktop computing with MATLAB, the Partial Least Squares (PLS) and Multivariate Image Analysis (MIA) Toolboxes, cited in biomedical imaging

research [24], [25], offer tensor decompositions and imaging customizations.

As Harrison and Joseph argue [26], the codesign of tensor algebra *and* software, what they call a tensor *framework*, has benefits. Codesign facilitates programmatic and computational efficiencies for solving a variety of model-based problems. In support, they cite Bader and Kolda's [27], [28] development of n -mode+ notation and the MATLAB Tensor Toolbox (MTT), also called the Tensor Toolbox for MATLAB. While Bader and Kolda contributed notation for decomposition constructs along with original software, others leveraged existing notations while contributing decomposition constructs and MATLAB toolboxes. These include structured data fusion (SDF) with Tensorlab, led by Sorber and De Lathauwer [29], [30], and the TT-Toolbox with the TT construct, by Osledets [31].

This paper proposes the Ricci-notation tensor (RT) framework for model-based approaches to imaging. A successor to Harrison and Joseph's numeric tensor (NT) framework [26], itself a complement to the EMV framework, the RT framework inherits their advantages. The proposed framework comprises an RT algebra and the RT software, defined as the RTToolbox plus MATLAB. Shared via MATLAB Central File Exchange synchronous with this publication, the RTToolbox parses the RT algebra, dispatching workhorse computation to the MATLAB kernel, with no dependencies on other toolboxes.

Both the NT and proposed RT algebras are index notations. The former exploited and extended Einstein notation, a subset of Ricci calculus notation [32]. However, the NT algebra is a multi-index notation not a single-index notation, as claimed. Using a dual-index notation, the RT algebra proves equally expressive as the NT algebra but aligns better with the dual-index notation of Ricci calculus. Additional extensions of the RT algebra support a variety of outer operations. Inspired by the broadcasting of EMV algebras, they remain grounded in an index notation fully compatible with Ricci calculus.

The NT software had variants. With LibNT, C/C++ end users expressed the NT algebra with programmatic and, especially, computational efficiency. With NTToolbox, comprising M-file and MEX wrappers for LibNT, MATLAB end users expressed the NT algebra with some programmatic and some computational penalties. The RT software has only a MATLAB variant, although this paper elaborates on its design in a C/C++-compatible way. As the toolbox comprises M-files only, no compilation or linking is required. Avoidance of MEX files and binaries also means that, as per MATLAB Central requirements [33], sharing is possible via File Exchange.

For its computational efficiency, the RT software leverages compiled unary and binary page-

wise functions introduced, in 2020 and 2022, to the MATLAB kernel. Of note, the kernel *pagewise* multiplication [34] resembles the LibNT *lattice* multiplication [26] introduced, in 2016, with the NT software. This paper elaborates on the lattice concept to facilitate RT left- and right-division using kernel functions. It also introduces *pagewise* concatenation, an interpreted function the RT software exploits to support N -ary tensor concatenation. Programmatic efficiency of the RT software is illustrated via software expressions cross-referenced to algebraic ones.

A tutorial example, to illustrate the RT algebra, is inspired by Sirbu *et al.*'s model-based research [35], [36], [37] for coronagraphy [38], which involves image and pupil planes, related by 2D discrete Fourier transforms (DFTs), and phase aberrations. The example adopts a simplified model. Starting with a Creative Commons public domain (CC0) image [39], called `Airy_disk_D65`, the impact of an optical system on a simulated image having an occulted star with nearby twin exoplanets is computed. The exoplanets become visible after model-based correction of an unknown phase aberration.

The rest of this paper is organized as follows. Section II introduces the RT algebra, contrasting it with the NT algebra. Section III illustrates the RT algebra's usefulness for a model-based approach involving 2D DFTs. Section IV summarizes the RT software, contrasting it with the NT software. Finally, Section V highlights contributions of this paper, this time with reference to selected details from Sections II to IV.

II. TENSOR ALGEBRA

In the proposed RT algebra, the mathematical objects of interest, called tensors, are scalars, vectors, and matrices of arbitrary degree, where degree is the number of dual, i.e., *covariant* or *contravariant*, indices. First, the value of exploiting and extending a dual-index Ricci notation is introduced in the context of scalars, even though these benefits also apply to nonscalars. Second, additional extensions of the algebra are summarized in the context of matrices and vectors.

A. Dual-Index Notation

The proposed RT algebra is introduced with reference to the NT algebra. Using an underline operator with what started out as a single-index Ricci notation, the NT algebra exploited the Einstein summation convention to support arbitrary mixtures of inner, entrywise, and outer products of N -degree scalars, not called N -dimensional arrays with reason. Use of the word

degree, or order, instead of dimensional, for the number of symbolic indices, is consistent with the Ricci calculus.

In the NT algebra, the underline operator prevents Einstein summation, resulting in entrywise products. Unnecessary complexity of the notation is demonstrable with simple examples, where indices are suppressed in inline math for readability. Consider the ternary inner product, x , and the ternary entrywise product, y , of three degree-one scalars, a , b , and c :

$$x = a_i b_i c_i, \quad (1)$$

$$y_i = a_{\underline{i}} b_{\underline{i}} c_{\underline{i}}. \quad (2)$$

For a variety of derivations, one needs to pair operands of N -ary products arbitrarily. This can be done with commutation and association identities, as follows for these examples:

$$x = b_i (a_{\underline{i}} c_{\underline{i}}), \quad (3)$$

$$y_i = b_{\underline{i}} (a_{\underline{i}} c_{\underline{i}}). \quad (4)$$

The underline operator stacks arbitrarily, meaning the character of an index can vary in a countable infinite way. This freedom has implications for the NT software. It also means the NT algebra is actually a multi-index Ricci notation.

Setting aside questions of constructivism, there is a simpler formalism, namely the extended dual-index notation of the RT algebra, that enjoys the accepted advantages of the NT algebra, for numeric purposes alone, while resolving the underline operator issue and laying a foundation for advanced geometric purposes. With this notation, inspired by the Ricci calculus of non-Euclidean geometry, any index has at most two characters: a *covariant*, or subscript, character; and a *contravariant*, or superscript, character. Whereas covariance and contravariance have specific geometric interpretations, specific support for advanced geometry is outside the scope of this paper.

With a conventional dual-index Ricci notation, the Einstein summation convention applies to each index that repeats twice where one index has a covariant character and the other a contravariant character. Other types of repeated indices are disallowed. This convention specifies inner products or, for one operand, contraction (summation) along each repeated index. With the RT algebra, indices of either character need not be unique. Repeated indices of the same character specify entrywise products or, for one operand, an attraction (selection) along each

repeated index. As with the NT algebra, unique indices across multiple operands specify outer products.

To support N -ary expressions having any combination of inner, entrywise, and outer products, as opposed to a hierarchy of binary products indicated with parentheses or a left-to-right precedence rule, what matters for the RT algebra is whether all repeats of an index do not or do have the same character. Returning to the ternary inner and entrywise examples, they are expressed and paired as follows, respectively:

$$x = a_i b_i c^i, \quad (5)$$

$$= b_i (a^i c^i), \quad (6)$$

$$y_i = a_i b_i c_i, \quad (7)$$

$$= b_i (a_i c_i). \quad (8)$$

As with the NT algebra, the RT algebra enjoys full associativity and commutativity for N -ary products with scalar operands of arbitrary degree. With either algebra, the character of one or more indices may change when altering associations.

Whereas inner products eliminate indices, tending to decrease the degree, outer products aggregate indices, tending to increase the degree. As they preserve repeated indices of the same character, entrywise products tend to maintain the degree. Outer products are easily expressed as follows:

$$z_{ijk} = a_i b_j c_k. \quad (9)$$

The examples of ternary inner, entrywise, and outer products are convenient for illustrating the known Ricci operation of contraction and an extended Ricci operation called attraction, both of which are unary operators that reduce degree:

$$x = z_{i\bar{i}\bar{i}}, \quad (10)$$

$$y_i = z_{i\bar{i}\bar{i}}. \quad (11)$$

An alternative way, namely an overscript bar, to specify a contravariant index is shown. Unlike with the underline of the NT algebra, each index of the RT algebra still has two possible characters. Stacked overscript bars collapse into one or zero overscript bars. To specify a contraction, at least one repeated index must have a complementary character.

With a superscript/subscript notation, often preferred in literature on non-Euclidean geometry, ambiguity is possible in expressions where not just an index but a tensor repeats. Consider the following apparently nonsensical statement:

$$y_i^j \neq y_i^j. \quad (12)$$

With the overscript bar notation, one could instead write a sensible inequality to represent the assymetry of a tensor:

$$y_{i\bar{j}} \neq y_{\bar{j}i}. \quad (13)$$

Contrast this with the dot-spacer notation of Ricci calculus, which allows superscripts for contravariant indices while clarifying index positions to resolve ambiguities as required:

$$y_i^{\cdot j} \neq y_i^{\cdot j}. \quad (14)$$

The RT algebra allows the superscript/subscript notation, with dot spacers as required, and the proposed overscript bar notation, where all indices are subscripts and dot spacers are never required. Another case of relevance is when permutations matter. They generalize transpositions, even to scalars. Consider a permuted copy, z , of a degree-two scalar, y :

$$z_i^{\cdot j} = y_i^{\cdot j}. \quad (15)$$

Removing the dot spacers here results in a sensical statement that, however, does not specify a numerical permutation:

$$z_i^j = y_i^j. \quad (16)$$

The number of possible permutations grows with the factorial of degree. Context determines if they matter to a model.

Mixtures of inner, entrywise, and outer products, and ways in which to rearrange them, are significant to CP derivations like those used to illustrate the NT algebra. Consider the following key step of a degree-three CP derivation, which uses the RT overscript bar notation to clarify index position and inner parentheses to group for asymptotic efficiency:

$$u_{i\bar{\ell}} = ((v_{j\ell}v_{\bar{j}\ell'})\overline{(w_{k\ell}w_{\bar{k}\ell'})})\backslash(a_{ijk}v_{\bar{j}\ell'}\overline{w_{\bar{k}\ell'}}). \quad (17)$$

As in the EMV algebra, a left (or right) division implies the solution to a linear system. In this case, it is as follows:

$$(v_{j\ell}v_{\bar{j}\ell'}\overline{w_{k\ell}w_{\bar{k}\ell'}})u_{i\bar{\ell}} = a_{ijk}v_{\bar{j}\ell'}\overline{w_{\bar{k}\ell'}}. \quad (18)$$

Iterating the key step and others like it, a degree-three scalar, a , decomposes into three degree-two factors, u , v , and w :

$$a_{ijk} = \sigma \ell u_{i\bar{\ell}} v_{j\bar{\ell}} w_{k\bar{\ell}}, \quad (19)$$

where the additional degree-one factor, σ , represents singular values, and where each degree-two factor obeys identities.

Previously, using the multi-index notation of the NT algebra, a novel derivation of the CP key step was provided as a tutorial example. As the same would be possible with the extended dual-index notation of the RT algebra, consider instead a difference between the NT and RT algebras concerning division, in the context of a simpler version of the CP key step:

$$u_{i\bar{\ell}} = A_{\ell\ell'} \setminus b_{i\ell'}, \quad (20)$$

$$A_{\ell\ell'} u_{i\bar{\ell}} = b_{i\ell'}. \quad (21)$$

Provided that each index, in the denominator operand of a division, changes to its complement, the RT algebra is equally consistent as the NT algebra for implied linear systems.

With MATLAB's implied EMV algebra, left/right division is equivalent to inversion or pseudo-inversion of the denominator operand followed by left/right multiplication. With the RT algebra, as with the NT algebra, there are multiple ways in which each index of a high-degree denominator operand may participate in a linear system, whether fully ranked or not. Absent the linear system context, fully specified by a left/right division, an inversion or pseudo-inversion of a denominator operand is ambiguous. Therefore, the RT algebra favours binary division expressions over a complicated scheme presented with the NT algebra to uniquely specify unary inverses.

In general, (partial) differentiation is explainable as the limiting solution of a linear system involving finite differences. The linear system may have an arbitrary mix of inner, entrywise, and outer products. Thus, (partial) differentiation rules for the RT algebra inherit observations made in the context of linear systems. To ensure consistency in formulations involving differentials, each index in the denominator operand of a differential changes to its complement when evaluated.

B. Additional Extensions

Like the NT algebra, the RT algebra supports nonscalars having indices, i.e., vectors and matrices of nonzero degree. In this paper, scalars are typeset with a plain italics font and

nonscalars with a bold Roman font. When the degree is nonzero, indices are indicated in display math. Indices are suppressed in inline math where possible due to context.

In general, the product of two nonscalars is noncommutative, which limits associativity for N -ary products. Consider a degree-two product, \mathbf{C} , of degree-two matrices, \mathbf{A} and \mathbf{B} , where columns of the first operand undergo an inner product with rows of the second operand, and where indices of the operands express entrywise products as per character:

$$\mathbf{C}_{i\bar{j}} = \mathbf{A}_{i\bar{j}}\mathbf{B}_{i\bar{j}}. \quad (22)$$

As rows and columns of an operand may be converted to and from symbolic indices, there is always an equivalent expression, with scalar operands of higher degree, that is fully commutative and, for N -ary products, fully associative:

$$c_{sti\bar{j}} = a_{s\bar{r}i\bar{j}}b_{rti\bar{j}}, \quad (23)$$

$$= b_{rti\bar{j}}a_{s\bar{r}i\bar{j}}. \quad (24)$$

Here, first and second indices of scalar operands correspond to rows and columns, respectively, of nonscalar operands. For an N -ary product of any-degree scalars, the operand sequence may be rearranged arbitrarily. This is not possible, in general, for an equivalent N -ary product of degree-zero matrices.

The binary product is reused to illustrate how a contraction or attraction is replaceable with an inner or entrywise operation across two operands with attention to index characters:

$$t = \text{tr } \mathbf{C}_{i\bar{i}}, \quad (25)$$

$$= \text{tr } \mathbf{A}_{ii}\mathbf{B}_{i\bar{i}}, \quad (26)$$

$$\mathbf{d}_i = \text{diag } \mathbf{C}_{ii}, \quad (27)$$

$$= \text{diag } \mathbf{A}_{ii}\mathbf{B}_{i\bar{i}}. \quad (28)$$

Because of their resemblance to contraction and attraction, these examples include the trace operator, tr , of MV algebra, and the main-diagonal operator, diag , of EMV algebra, which concern only the rows and columns of an operand.

Inner products help justify why each enclosed index changes to its complement in a (conjugate) transposition. Consider these equivalent expressions for the Euclidean norm squared, $\|\mathbf{x}\|^2$, of an any-degree column vector, \mathbf{x} , having all-contravariant indices and possibly-complex entries:

$$\|\mathbf{x}^{\mathbf{k}}\|^2 = (\bar{\mathbf{x}}^{k_1 k_2 \dots k_D})^T \mathbf{x}^{k_1 k_2 \dots k_D}, \quad (29)$$

$$= (\mathbf{x}^{\mathbf{k}})^* \mathbf{x}^{\mathbf{k}}, \quad (30)$$

$$= \bar{\mathbf{x}}_{k_1 k_2 \dots k_D}^T \mathbf{x}^{k_1 k_2 \dots k_D}, \quad (31)$$

$$= \mathbf{x}_{\mathbf{k}}^* \mathbf{x}^{\mathbf{k}}, \quad (32)$$

where multiple indices in sequence may be represented as an index vector. An overscript bar on a tensor, as opposed to an index, indicates complex conjugation of tensor entries.

Unlike the NT algebra, the RT algebra supports outer additions, subtractions, concatenations, and relations. The unifying idea is that any tensor of one degree may be expanded to an equivalent tensor of higher degree via an outer product with a unit tensor of the difference degree. Consider the following equations and relation, which consistently employ a degree-two matrix, \mathbf{A} , four degree-one column-vectors, $\mathbf{1}$, \mathbf{b} , \mathbf{c} , and $\mathbf{1}$, and an entrywise absolute-value operation, $|\cdot|$:

$$\mathbf{A}_i^j = \mathbf{1}_i (\mathbf{b}_j)^T + |\mathbf{c}_i| (\mathbf{1}_j)^T, \quad (33)$$

$$= \begin{bmatrix} \mathbf{1}_i & |\mathbf{c}_i| \end{bmatrix} \begin{bmatrix} (\mathbf{b}_j)^T \\ (\mathbf{1}_j)^T \end{bmatrix}, \quad (34)$$

$$\mathbf{A}_i^j \geq \mathbf{1}_i (\mathbf{b}_j)^T. \quad (35)$$

Whereas the NT algebra would require the with-unit outer products explicitly, as per Ricci notation, the RT algebra allows them implicitly, an extension of the Ricci notation:

$$\mathbf{A}_i^j = (\mathbf{b}_j)^T + |\mathbf{c}_i|, \quad (36)$$

$$= \begin{bmatrix} \mathbf{1} & |\mathbf{c}_i| \end{bmatrix} \begin{bmatrix} (\mathbf{b}_j)^T \\ \mathbf{1}^T \end{bmatrix}, \quad (37)$$

$$\mathbf{A}_i^j \geq (\mathbf{b}_j)^T. \quad (38)$$

The missing outer products are implied by what may be called natural algebra, setting aside index character complexity.

For an easier-to-read example, this time with scalars, of the naturalness of the proposed RT algebra, consider a logarithmic model for the digital response or output, y , of a wide-dynamic-range image sensor to a uniform stimulus or input, x :

$$y_{ij} = a_j + b_j \ln(c_j + x_i) + \epsilon_{ij}. \quad (39)$$

Offset, gain, and bias parameters, a , b , and c , vary with pixel index, j , but not with illumination index, i . In addition to such structural noise, the model accounts for temporal and quantization noise, ϵ . A parseable expression of RT algebra, the model implies three with-unit outer products, an entrywise function, and a mixed (entrywise-and-outer) product.

Outer RT operations resemble broadcasting, popularized by the implied EMV algebra of Python+NumPy, but are modelled with a symbolic index notation. One advantage of index-based outer operations is that they express broadcasting in a way that would look familiar even to high-school, or A-level, students. This attests further to the value of the RT algebra for model-based approaches, which favour human intelligence, as opposed to learning-based approaches, which favour machine intelligence. By design, the RT algebra complements the implied EMV algebra of MATLAB. Outer RT operations naturally extend broadcasting capabilities of the latter.

With MATLAB's implied EMV algebra, an inner product of two matrices is representable as a product of vectors, with one conjugate transposed, after a vectorization is applied to each matrix. There is no MATLAB operator for an inner product of matrices, although there is one for an entrywise, or Hadamard, product of the same. In the RT algebra, these operators may be denoted with a bullet and a circle, respectively.

Although EMV algebra includes entrywise concatenation along non-row/column dimensions, computable in MATLAB via the kernel `cat` function, the RT algebra offers a way to model it with symbolic indices, a model generalizable to outer concatenation. Consider an outer concatenation of degree-two matrices, \mathbf{A} and \mathbf{B} , along a common symbolic index:

$$\mathbf{C}_{ijk} = \text{cat}_j\{\mathbf{A}_{ij}, \mathbf{B}_{jk}\}, \quad (40)$$

$$= \delta_j^\ell (\alpha_\ell^j \mathbf{A}_{ij} + \beta_\ell^j \mathbf{B}_{jk}). \quad (41)$$

The degree-three result, \mathbf{C} , is modelled with the help of degree-two scalars, α and β , each

similar to a degree-two Dirac symbol, δ , commonly used for index substitution:

$$\alpha_\ell^j \equiv \begin{cases} 1, & \ell = j, \\ 0, & \text{otherwise,} \end{cases} \quad (42)$$

$$\beta_\ell^j \equiv \begin{cases} 1, & \ell = J_1 + j, \\ 0, & \text{otherwise.} \end{cases} \quad (43)$$

The constant, J_1 , is the dimension size of the symbolic index, j , in the first operand, A . With additional constants, $J_1 + J_2$, etc., the model is generalizable to N -ary concatenation.

III. TUTORIAL EXAMPLE

This section illustrates the RT algebra via a tutorial example, called the phase aberration correction. To facilitate a summary of the model-based simulation, motivated by an exoplanet imaging instrument called a coronagraph, results are presented first. Details of the optimization problem, like its objective function, are formulated using the RT algebra and (inverse) DFT operators. Leveraging (inverse) fast Fourier transforms (FFTs), an asymptotically efficient solution is proposed.

A. Simulation Results

Figure 1 displays, after each pixel value is squared and rounded, the *ground-truth* image of the simulation. The image, a representation of electric field pattern, is derived from a CC0-licensed image, `Airy_disk_D65`, itself a simulation of a focused spot of white light passing through a circular aperture and lens. Rings in the focal or image plane arise due to diffraction. The figure also displays a *mask* image, with an annular foreground and an opaque background. Using the mask to model a coronagraph very simply, a bright spot centered in `Airy_disk_D65` is fully blacked out, representing an occulted star. Similarly, an outer symmetric region, comprising weaker diffraction rings, is blacked out.

After the masking, filled circles introduced into the annular foreground simulate twin exoplanets. The result, treated as ground-truth, has 401×401 pixels, same as the *source* image, `Airy_disk_D65`. Moreover, after converting from class `uint8` to class `double`, and from true colour to grayscale, an entrywise square root was applied in making the ground-truth image. Using bicubic or nearest-neighbour interpolation, respectively, ground-truth and mask images are

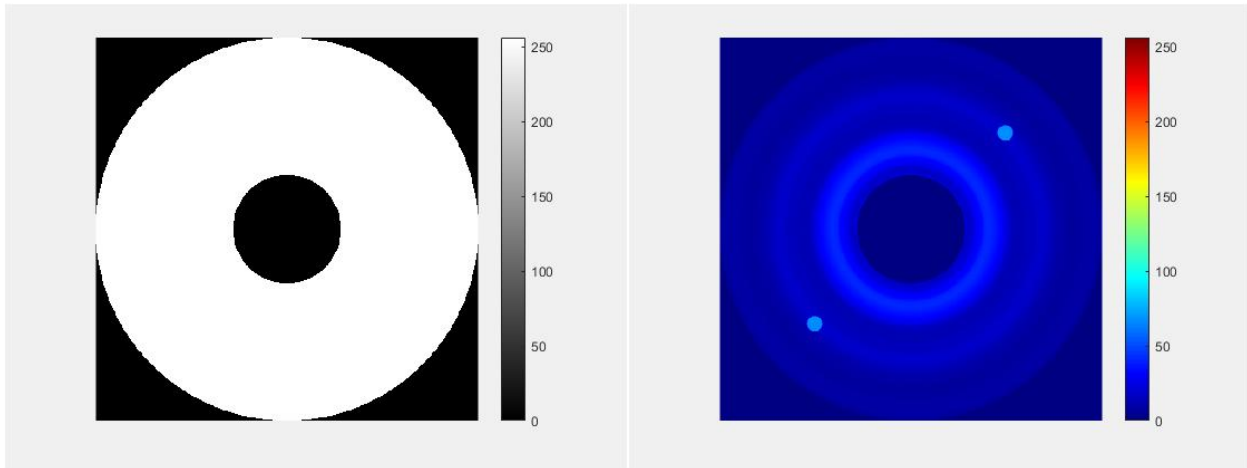


Fig. 1. Simulated mask and ground-truth images (original scale). After simulating twin exoplanets (small spots), the entrywise square root of a masked image called `Airy_disk_D65`, courtesy of Wikipedia [39], is converted to grayscale to make a ground-truth image (right). Before display, pixel values are squared and rounded. A mask (left) occults the large bright spot, representing a star, in `Airy_disk_D65` and a symmetric region beyond a certain radius.

downsampled or upsampled as needed, to vary dimension sizes equally for simulation purposes. The mask is of class `logical`.

The ground-truth image does not exhibit a phase aberration. To simulate an *aberrated* image, a random phase offset is introduced in the Fourier domain, often called the pupil plane in the context of exoplanet imaging. Because pixel values in the image plane, also called the inverse Fourier domain, must be real, the phase offset is thereby constrained to obey the required symmetry. Notwithstanding a few entries, such as the DC value, each entry of the phase offset, an image-like matrix, belongs to a uniform distribution of $-\pi$ to $+\pi$ radians.

Figure 2 shows two images that best illustrate the tutorial example. One is the input *aberrated* image and the other is the output *corrected* image. Prior to display, each pixel value is squared and rounded. Starting with an initial guess of the phase offset, an optimization yields a corrected image, approaching the ground-truth, through iteration. The procedure updates the phase offset by minimizing a scalar sum squared error (SSE), which is plotted. The SSE aggregates deviations in the image plane alone. A corrected image should have nonnegative values in the foreground and zero values in the background.

The initial guess of the phase offset is an all-zero matrix. With it, the optimization converges toward a local minimum at which, although the computed phase offset differs (not shown) from the true one, the problem is adequately solved, at least in terms of diffraction ring and exoplanet

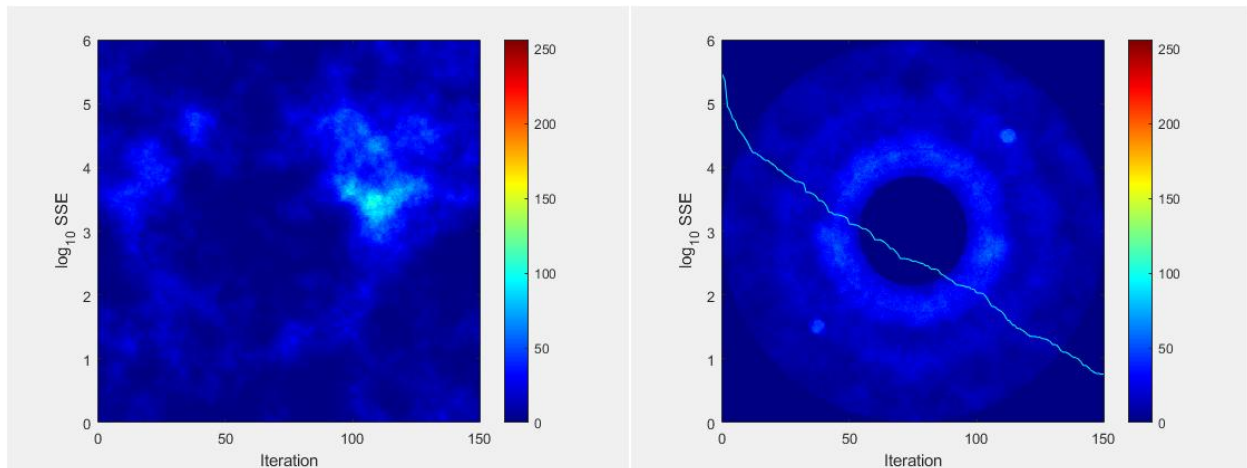


Fig. 2. Model-based approach to address a phase aberration. Initial (left) and final (right) iterations of an optimization are shown. An unknown phase offset in the pupil plane of a simulated optical system model is corrected by minimization of an image-plane SSE. Nonzero pixels outside an annulus, and negative pixels inside it, define the SSE. Diffraction rings and twin exoplanets become visible in an annular foreground as the phase aberration is corrected.

visibility.

An accurate and efficient SSE computation is required for dimension sizes of interest, given a phase offset guess, plus the same for first and second SSE derivatives with respect to the offset. Otherwise, the optimization either does not converge at all, due to numerical errors in automatic approximations of the first derivative, the gradient, or does not converge in reasonable time, due to higher-order curvature not captured without either the second derivative, the Hessian, or sufficient second-derivative information, a Hessian multiply function (HMF). Thanks to the RT algebra, accurate and efficient SSE, gradient, and HMF computations are possible.

From a practical perspective, a computing problem is solveable only if it requires a reasonable amount of processing time, measurable in seconds (s), and a reasonable amount of memory space, measurable in bytes (B) of random access memory (RAM), to solve it. For desktop computing, reasonable space means the RAM of a personal computer (PC) suffices for the image resolution, 401×401 pixels, at hand. Reasonable time means a fractional second per iteration suffices on the PC, a Dell Latitude E7450 with 8 GB of RAM, for the same.

Figures 3 and 4 report the compute time and memory space required, versus the number of pixels, to determine the SSE only, the SSE-and-gradient, and the HMF for one iteration. Compute time is measured using MATLAB's `tic` and `toc` functions, averaged over multiple iterations with a `for` loop. Using MATLAB's `whos` and `sum` functions, invoked carefully with

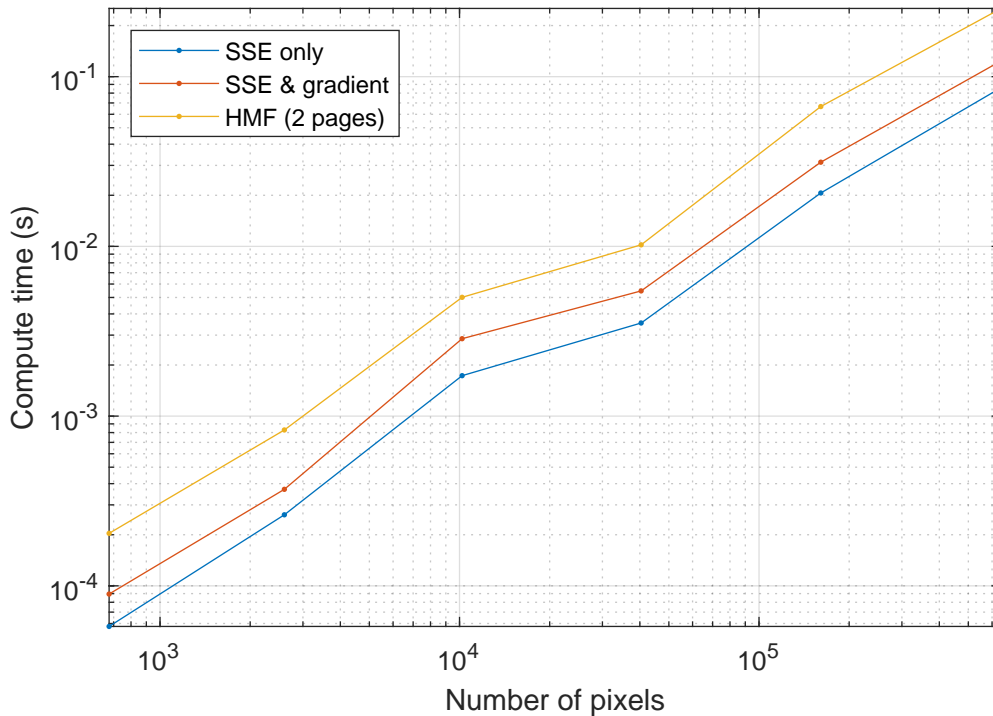


Fig. 3. Compute time for tutorial example (multiple scales). For an $M \times N$ problem, computing first (gradient) and second (HMF) derivatives of the scalar SSE, with respect to an $M \times N$ matrix (phase offset in the Fourier domain), is asymptotically equivalent to computing the SSE alone, thanks to time efficiencies of a model-based solution derived with the RT algebra.

negligible overhead, the same implementation totals and returns memory space, which is reused each iteration.

Like the gradient, the HMF is not required every iteration. When the HMF is computed, its time-and-space requirements per page, in the worst case, are multiplied by an unspecified number of pages. This number (about two), automatically chosen and not reported by the optimization routine, appeared to be small enough for the SSE to be suitably minimized, as shown in Figure 2, in reasonable time and space overall.

B. Scalar Error

The tutorial example input is an $M \times N$ *aberrated* image, \mathbf{X}^a , where before display each pixel value is squared and rounded. The output is an estimate of the *ground-truth* image, \mathbf{X}^t , having the same dimension sizes. One defines a scalar SSE function in the image plane, an inverse Fourier domain, with a model. Corresponding to an SSE minimum, a candidate solution to the problem is called a *corrected* image, $\hat{\mathbf{X}}^t$.

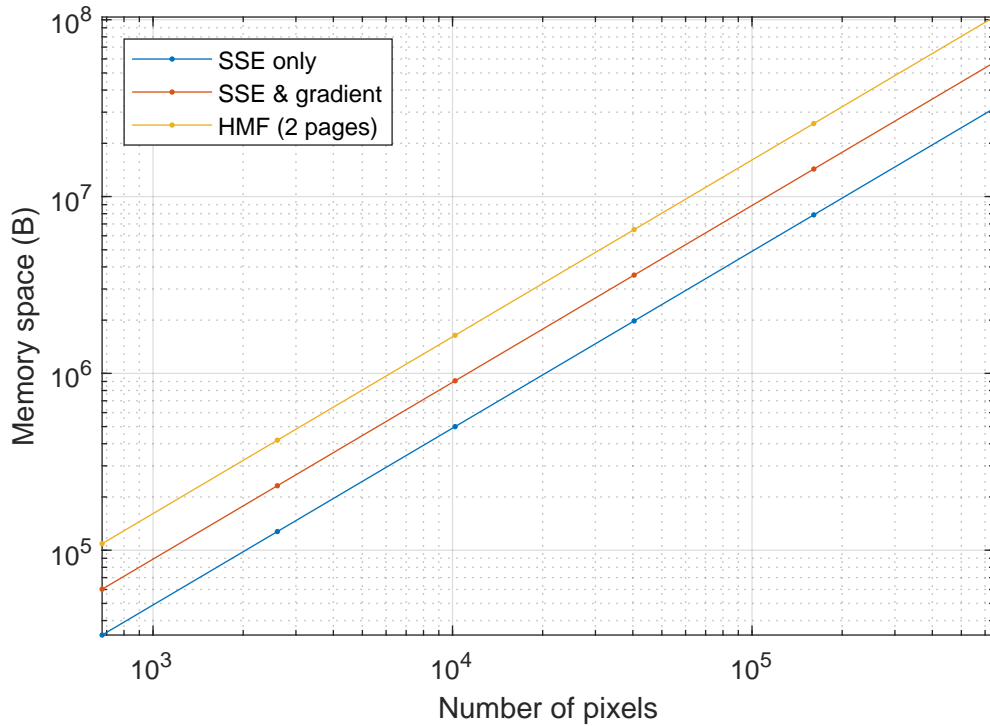


Fig. 4. Memory space for tutorial example (multiple scales). For an $M \times N$ problem, computing first (gradient) and second (HMF) derivatives of the scalar SSE, with respect to an $M \times N$ matrix (phase offset in the Fourier domain), is asymptotically equivalent to computing the SSE alone, thanks to space efficiencies of a model-based solution derived with the RT algebra.

To formulate the ground-truth image, *unknown* in practice, one models an optical system, as follows, with *unknown* phase offset, $\Delta\Phi$, in the pupil plane, a Fourier domain. Here, \mathbf{Y}^a is the 2D DFT of \mathbf{X}^a and \mathbf{X}^t is the inverse 2D DFT of \mathbf{Y}^t :

$$\mathbf{Y}^a = \mathbf{U}\mathbf{X}^a\mathbf{V}^T, \quad (44)$$

$$\Phi^t = \angle\mathbf{Y}^a + \Delta\Phi, \quad (45)$$

$$\mathbf{Y}^t = |\mathbf{Y}^a| \circ \exp(j\Phi^t), \quad (46)$$

$$\mathbf{X}^t = \frac{1}{MN} \bar{\mathbf{U}}^T \mathbf{Y}^t \bar{\mathbf{V}}. \quad (47)$$

If the phase offset, $\Delta\Phi$, is *known* then the ground-truth image, \mathbf{X}^t , is easily found from the magnitude and phase, $|\mathbf{Y}^a|$ and $\angle\mathbf{Y}^a$, of the aberrated image's 2D DFT, always *known*.

The 1D DFT operators, \mathbf{U} and \mathbf{V} , model an (inverse) 2D DFT via matrix multiplication. For an $M \times N$ matrix, \mathbf{X} , in the image plane and its $M \times N$ counterpart, \mathbf{Y} , in the pupil plane, the operators are matrices having dimension sizes $M \times M$ and $N \times N$, respectively. Each entry

of the first operator, \mathbf{U} , is a complex number whose exponent varies with the row and column index of an integer outer product, \mathbf{K} , modulo M :

$$\mathbf{U} = \exp(-j2\pi\mathbf{K}/M), \quad (48)$$

$$\mathbf{K} = \mathbf{k}^T \mathbf{k} \pmod{M}, \quad (49)$$

$$\mathbf{k} = \begin{bmatrix} 0 & \dots & M-1 \end{bmatrix}. \quad (50)$$

The second operator, \mathbf{V} , is defined similarly. The conjugate transpose of an operator gives its inverse, where a dimension size, M or N , provides the scale needed for an identity:

$$\frac{1}{M} \bar{\mathbf{U}}^T \mathbf{U} = \mathbf{I}. \quad (51)$$

By the problem definition, the ground-truth image, \mathbf{X}^t , is real, and so is the aberrated image, \mathbf{X}^a . Thus, the complex-valued 2D DFT, \mathbf{Y}^a , exhibits a phase symmetry. The 2D DFT of the ground-truth image, \mathbf{Y}^t , differs only in phase due to an offset. Therefore, for the ground-truth image to be real, there is an implied symmetry constraint on the phase offset, $\Delta\Phi$. Discarding the imaginary part, after an inverse DFT, deals with round-off error issues that may arise in practice:

$$\mathbf{X}^t = \frac{1}{MN} \text{Re}\{\bar{\mathbf{U}}^T \mathbf{Y}^t \bar{\mathbf{V}}\}. \quad (52)$$

To correct the aberration, one requires *a priori* information, in this case *occultation*. The ground-truth image, when occulted, defines background and foreground errors, \mathbf{X}^b and \mathbf{X}^f , that equal zero if the phase offset, $\Delta\Phi$, is corrected:

$$\mathbf{X}^b = \mathbf{W}^b \circ \mathbf{X}^t, \quad (53)$$

$$\mathbf{X}^f = \mathbf{W}^f \circ \mathbf{X}^t, \quad (54)$$

$$\mathbf{W}^f = (\mathbf{1} - \mathbf{W}^b) \circ u(-\mathbf{X}^t). \quad (55)$$

For an annular occulter, with no loss of generality, the background mask, \mathbf{W}^b , is zero at each pixel inside the annulus and one outside it. Note the use of entrywise products.

Background and foreground errors test for deviant pixel values, where entries of background and foreground masks, \mathbf{W}^b and \mathbf{W}^f , are one, respectively. The masks are not complementary because a step function, u , filters out nonnegative values in the foreground. However, as the masks are orthogonal, they may be added to help formulate a single error image:

$$\mathbf{X}^e = (\mathbf{W}^b + \mathbf{W}^f) \circ \mathbf{X}^t. \quad (56)$$

If the error image, \mathbf{X}^e , deviates from a zero matrix then the phase offset, $\Delta\Phi$, requires correction. Thus, the SSE is defined as the inner product, E , of the error image with itself:

$$E = \bar{\mathbf{X}}^e \bullet \mathbf{X}^e. \quad (57)$$

C. Gradient Matrix

At a minimum of the SSE, its gradient, ∇E , with respect to the phase offset, $\Delta\Phi$, vanishes. To avoid differentiating matrices with respect to a matrix, the model employs a degree-two scalar version, $\Delta\phi^{ij}$, of the phase offset instead:

$$\nabla E = (g^{ij} + \bar{g}^{ij}) \mathbf{e}_i \mathbf{e}_j^T, \quad (58)$$

$$g_{ij} = \frac{\partial \bar{\mathbf{X}}^e}{\partial \Delta\phi^{ij}} \bullet \mathbf{X}^e, \quad (59)$$

$$\Delta\Phi = \Delta\phi^{ij} \mathbf{e}_i \mathbf{e}_j^T. \quad (60)$$

Degree-one basis operators, \mathbf{e}_i and \mathbf{e}_j , model scalar conversion. Each is a column vector with one nonzero, equal to one, the row of which corresponds to the index. When the error image, \mathbf{X}^e , is zeroed, the gradient of the SSE is zeroed.

The gradient matrix, ∇E , appears to depend on an infinite-valued Dirac delta function, δ , the derivative of a Heaviside step function, u , which is discontinuous at the origin. First, the partial derivative of the error image, \mathbf{X}^e , is expanded:

$$\frac{\partial \mathbf{X}^e}{\partial \Delta\phi^{ij}} = \frac{\partial \mathbf{W}}{\partial \Delta\phi^{ij}} \circ \mathbf{X}^t + \mathbf{W} \circ \frac{\partial \mathbf{X}^t}{\partial \Delta\phi^{ij}}, \quad (61)$$

where the sum, \mathbf{W} , of background and foreground masks, \mathbf{W}^b and \mathbf{W}^f , is given a symbol. A problematic partial derivative term, which could be infinite valued, is expanded next:

$$\frac{\partial \mathbf{W}}{\partial \Delta\phi^{ij}} \circ \mathbf{X}^t = (\mathbf{1} - \mathbf{W}^f) \circ \frac{\partial u(-\mathbf{X}^t)}{\partial \Delta\phi^{ij}} \circ \mathbf{X}^t, \quad (62)$$

$$\frac{\partial u(-\mathbf{X}^t)}{\partial \Delta\phi^{ij}} = \delta(-\mathbf{X}^t) \circ -\frac{\partial \mathbf{X}^t}{\partial \Delta\phi^{ij}}. \quad (63)$$

Fortunately, the problematic derivative is zero. Using associative and commutative properties of entrywise matrix products, with even and sifting properties of an entrywise Dirac delta function, the following identity holds for any matrix, \mathbf{X}^t :

$$\delta(-\mathbf{X}^t) \circ \mathbf{X}^t = \mathbf{0}. \quad (64)$$

After eliminating the problematic derivative, a complex-valued degree-two scalar, g_{ij} , is rewritten and simplified as follows, partly because $\mathbf{W} \circ \mathbf{W}$ happens to equal \mathbf{W} :

$$g_{ij} = \left(\mathbf{W} \circ \frac{\partial \bar{\mathbf{X}}^t}{\partial \Delta \phi^{ij}} \right) \bullet \mathbf{X}^e, \quad (65)$$

$$= \frac{\partial \bar{\mathbf{X}}^t}{\partial \Delta \phi^{ij}} \bullet (\mathbf{W} \circ \mathbf{X}^e), \quad (66)$$

$$= \frac{\partial \bar{\mathbf{X}}^t}{\partial \Delta \phi^{ij}} \bullet \mathbf{X}^e. \quad (67)$$

Required for simplification, a commutation and association identity is derived by considering an equivalent scalar expression, having a mixture of entrywise and inner products:

$$g_{ij} = \left(w_{kl} \frac{\partial \bar{x}_{kl}^t}{\partial \Delta \phi^{ij}} \right) x_e^{kl}, \quad (68)$$

$$= \frac{\partial \bar{x}_{kl}^t}{\partial \Delta \phi^{ij}} (w^{kl} x_e^{kl}). \quad (69)$$

Subsequently, using the inverse DFT model, the partial derivative of the ground-truth image, \mathbf{X}^t , with respect to the phase offset, $\Delta \phi^{ij}$, may be expanded as follows:

$$\frac{\partial \mathbf{X}^t}{\partial \Delta \phi^{ij}} = \frac{1}{MN} \bar{\mathbf{U}}^T \frac{\partial \mathbf{Y}^t}{\partial \Delta \phi^{ij}} \bar{\mathbf{V}}, \quad (70)$$

$$\frac{\partial \mathbf{Y}^t}{\partial \Delta \phi^{ij}} = \mathbf{Y}^t \circ \mathcal{J} \frac{\partial \Phi^t}{\partial \Delta \phi^{ij}}, \quad (71)$$

$$\frac{\partial \Phi^t}{\partial \Delta \phi^{ij}} = \mathbf{e}_i \mathbf{e}_j^T. \quad (72)$$

Similar to the nonconjugate case, the partial derivative of the ground-truth image's conjugate, $\bar{\mathbf{X}}^t$, with respect to the phase offset, $\Delta \phi^{ij}$, may be expressed as follows:

$$\frac{\partial \bar{\mathbf{X}}^t}{\partial \Delta \phi^{ij}} = \frac{-\mathcal{J}}{MN} \mathbf{U}^T (\bar{\mathbf{Y}}^t \circ \mathbf{e}_i \mathbf{e}_j^T) \mathbf{V}. \quad (73)$$

To simplify this expression, the enclosed matrix, \mathbf{Y}^t , converts to an equivalent degree-two scalar, y_{ij}^t , as follows:

$$\mathbf{Y}^t \circ \mathbf{e}_i \mathbf{e}_j^T = y_{ij}^t \mathbf{e}_i \mathbf{e}_j^T. \quad (74)$$

As a scalar, of any degree, may be factored out of a multi-operand product, the partial derivative simplifies:

$$\frac{\partial \bar{\mathbf{X}}^t}{\partial \Delta \phi^{ij}} = \frac{-\mathcal{J}}{MN} y_{ij}^t \mathbf{U}^T \mathbf{e}_i \mathbf{e}_j^T \mathbf{V}. \quad (75)$$

Thus, the degree-two scalar, g_{ij} , may be expressed in terms of another degree-two scalar, denoted y_{ij}^e , as follows:

$$g_{ij} = \frac{-J}{MN} \bar{y}_{ij}^t y_{ij}^e, \quad (76)$$

$$y_{ij}^e = (\mathbf{U}^T \mathbf{e}_i \mathbf{e}_j^T \mathbf{V}) \bullet \mathbf{X}^e. \quad (77)$$

By replacing the basis operators, \mathbf{e}_i and \mathbf{e}_j , the 1D DFT operators, \mathbf{U} and \mathbf{V} , and the error image, \mathbf{X}^e , with equivalent degree-two scalars, including Dirac operators, δ , the following reformulation arises, thanks to the RT algebra:

$$y_{ij}^e = (u_{\alpha k} \delta^{\alpha i} \delta^{\beta j} v_{\beta \ell}) x_e^{k\ell}, \quad (78)$$

$$= u_{ik} x_e^{k\ell} v_{j\ell}. \quad (79)$$

If each degree-two scalar, e.g., $x_e^{k\ell}$, is now replaced with an equivalent matrix, i.e., \mathbf{X}^e , a hidden 2D DFT reveals:

$$\mathbf{G} = \frac{-J}{MN} \bar{\mathbf{Y}}^t \circ \mathbf{Y}^e, \quad (80)$$

$$\mathbf{Y}^e = \mathbf{U} \mathbf{X}^e \mathbf{V}^T. \quad (81)$$

Hence, the matrix equivalent, \mathbf{G} , of the degree-two scalar, g_{ij} , is directly proportional to an entrywise product, in the Fourier domain with one operand conjugated, of the ground-truth image, \mathbf{X}^t , and the error image, \mathbf{X}^e . As the gradient matrix, ∇E , equals twice the real part, $\text{Re}\{\mathbf{G}\}$, of this equivalent, its final formulation is relatively simple:

$$\nabla E = \mathbf{G} + \bar{\mathbf{G}}, \quad (82)$$

$$= \frac{2}{MN} \text{Im}\{\bar{\mathbf{Y}}^t \circ \mathbf{Y}^e\}. \quad (83)$$

D. Hessian Function

For the phase aberration correction problem, once the SSE and its gradient are formulated, one may attempt to construct a solution using an established routine, like `fminunc` from MATLAB's Optimization Toolbox. This function offers the user a choice between quasi-Newton and trust-region algorithms. Because the former proves too slow even on small-format test cases, all simulations employ the latter. With the quasi-Newton algorithm, the gradient is actually optional. With the trust-region algorithm, the gradient is required.

Asymptotically, it takes equal time and space to construct the SSE and gradient as the SSE alone. Using explicit DFT operators, either takes $O(M^2N + MN^2)$ time and $O(MN)$ space. Each DFT operator represents a Fourier transform, or its inverse, as matrix multiplication. One need not construct the operator, a useful formalism, as the FFT constructs a DFT faster. Using 2D FFTs, the SSE and gradient or the SSE only takes $O(MN \log MN)$ time and $O(MN)$ space.

Non-asymptotically, it takes longer to compute the SSE and gradient than it does to compute the SSE alone. Yet without the gradient, on small-format test cases, the trust-region algorithm was too slow. For medium and large-format test cases, even the benefit of an explicit first-order partial derivative, the gradient, was insufficient. For a practical solution, an implicit second-order partial derivative, an HMF, was needed. The RT algebra helps to formulate and simplify the desired HMF.

On one hand, the Hessian, \mathbf{H} , of the scalar SSE, E , is a degree-two matrix that requires at least $O(M^2N^2)$ space and, therefore, time to construct, even with FFT acceleration:

$$\mathbf{H}_{ij} = \frac{\partial \nabla E}{\partial \Delta \phi^{ij}}. \quad (84)$$

On the other hand, the HMF, \mathbf{F} , is a degree-one matrix that requires at least $O(MNP)$ space and time to construct, where the dimension size, P , refers to a third index, k , of the phase offset, $\Delta \varphi$, a degree-three, not a degree-two, scalar here:

$$\mathbf{F}_k = \mathbf{H}_{ij} \Delta \varphi_k^{ij}. \quad (85)$$

According to details of the trust-region algorithm, the HMF is computed occasionally only after a gradient computation. Using available matrices, \mathbf{Y}^t and \mathbf{Y}^e , of the gradient computation, the HMF is readily expressed after expansion:

$$\mathbf{F}_k = \frac{2}{MN} \text{Im} \left\{ \frac{\partial \bar{\mathbf{Y}}^t}{\partial \Delta \phi^{ij}} \circ \mathbf{Y}^e + \bar{\mathbf{Y}}^t \circ \frac{\partial \mathbf{Y}^e}{\partial \Delta \phi^{ij}} \right\} \Delta \varphi_k^{ij}, \quad (86)$$

$$= \frac{2}{MN} \text{Im} \{ \Delta \bar{\mathbf{Y}}_k^t \circ \mathbf{Y}^e + \bar{\mathbf{Y}}^t \circ \Delta \mathbf{Y}_k^e \}, \quad (87)$$

where HMF components, $\Delta \bar{\mathbf{Y}}^t$ and $\Delta \mathbf{Y}^e$, represent a sequence of 2D DFT increments, with one of them conjugated. The first HMF component, $\Delta \mathbf{Y}_k^t$, is also readily formulated:

$$\Delta \mathbf{Y}_k^t = (\mathbf{Y}^t \circ j \mathbf{e}_i \mathbf{e}_j^T) \Delta \varphi_k^{ij}, \quad (88)$$

$$= j \mathbf{Y}^t \circ \Delta \Phi_k, \quad (89)$$

$$\Delta \Phi_k = \Delta \varphi_k^{ij} \mathbf{e}_i \mathbf{e}_j^T, \quad (90)$$

where the degree-three scalar, $\Delta\varphi$, is replaced with an equivalent degree-one matrix, $\Delta\Phi$. The incremental time and space cost of constructing this conversion, if it were actually needed beyond a formalism, can be made practically zero.

The second HMF component, $\Delta\mathbf{Y}^e$, is partially formulated by revealing a sequence of 2D DFTs as follows:

$$\Delta\mathbf{Y}_k^e = \left(\mathbf{U} \frac{\partial \mathbf{X}^e}{\partial \Delta\phi^{ij}} \mathbf{V}^T \right) \Delta\varphi_k^{ij}, \quad (91)$$

$$= \mathbf{U} \Delta\mathbf{X}_k^e \mathbf{V}^T, \quad (92)$$

$$\Delta\mathbf{X}_k^e = \left(\mathbf{W} \circ \frac{\partial \mathbf{X}^t}{\partial \Delta\phi^{ij}} \right) \Delta\varphi_k^{ij}, \quad (93)$$

$$= \mathbf{W} \circ \Delta\mathbf{X}_k^t. \quad (94)$$

To complete the formulation, a sequence of inverse 2D DFTs of the first HMF component, $\Delta\mathbf{Y}_k^t$, is revealed:

$$\Delta\mathbf{X}_k^t = \left\{ \frac{J}{MN} \bar{\mathbf{U}}^T (\mathbf{Y}^t \circ \mathbf{e}_i \mathbf{e}_j^T) \bar{\mathbf{V}} \right\} \Delta\varphi_k^{ij}, \quad (95)$$

$$= \frac{J}{MN} \bar{\mathbf{U}}^T (\mathbf{Y}^t \circ \Delta\Phi_k) \bar{\mathbf{V}}, \quad (96)$$

$$= \frac{1}{MN} \bar{\mathbf{U}}^T \Delta\mathbf{Y}_k^t \bar{\mathbf{V}}. \quad (97)$$

Thanks to the RT algebra, the HMF asymptotically requires, with 2D FFTs, $O(MNP \log MN)$ time and $O(MNP)$ space to compute. This asymptotic complexity is directly proportional by a factor, P , to that of the gradient. The incremental time-and-space complexity of computing the HMF, \mathbf{F} , with the gradient, ∇E , is $O(1)$ asymptotically if P , which depends on the optimization routine, `fminunc`, is bounded above.

IV. TENSOR SOFTWARE

Table I introduces the RTToolbox. Together with the classes and functions of the MATLAB kernel, compiled or interpreted, the RTToolbox defines the RT software. First, this section offers a design overview of `tensor` objects. Next, it summarizes `index` objects, which play a critical role in enabling a dual-index notation. Finally, key problems and solutions, contrasted with closest equivalents of the NT software, are summarized for unary, binary, and N -ary operations.

TABLE I

COMPOSITION OF THE RTTOOLBOX. THE RT SOFTWARE IS DEFINED AS THE RTTOOLBOX, COMPRISING `TENSOR` AND `INDEX` CLASSES, PAGEWISE FUNCTIONS, AND UNIT TESTS, AND THE MATLAB KERNEL. TOGETHER, THEY NATURALLY EXPRESS AND COMPUTE THE RT ALGEBRA. THERE ARE NO DEPENDENCIES ON OTHER TOOLBOXES (OR LIBRARIES).

M-file	Summary	Note
<code>tensor.m</code>	Definition of <code>tensor</code> objects	Table II
<code>tensorTest.m</code>	Tests of <code>tensor</code> objects	Table III
<code>index.m</code>	Definition of <code>index</code> objects	Table IV
<code>indexTest.m</code>	Tests of <code>index</code> objects	Table V
<code>pagetrace.m</code>	Pagewise trace function	Figure 5
<code>pagediag.m</code>	Pagewise diag function	-
<code>pagehorzcat.m</code>	Pagewise horzcat function	Figure 5
<code>pagevertcat.m</code>	Pagewise vertcat function	-
<code>pagecat.m</code>	Pagewise cat function	-

A. Tensor Objects

Table II summarizes the `tensor` class. Apart from the first group, constructor aside, and `isequal`, all methods return a `tensor` object. Table III presents excerpts, cross-referenced to equations, from selected unit tests of class `tensor`.

A `tensor` object has two protected properties, `indices` and `entries`, which the `index` and `entry` methods offer a copy of, respectively. The `indices` property is a row vector, possibly empty, of class `index`. The `entries` property must be a non-tensor array, an MDA, usually of class `double` or `logical`, the only classes represented in the unit tests.

For a `tensor` object, the `degree` method returns the number of indices, i.e., the `numel` of the `indices` property, and the `ndims` methods returns the number of dimensions, i.e., the `ndims` of the `entries` property. Because first and second dimensions are MDA rows and columns, the `degree` is at least two less than the `ndims` of a `tensor` object.

The one-argument constructor returns a `tensor` object, whose `entries` and `degree` equal the non-tensor argument and its `ndims` minus two. A corresponding `index` object is constructed and assigned to the `indices`. A zero-argument, or default, constructor returns a `tensor` object of degree zero with empty `entries` and `indices`.

The last constructor variant enables a `tensor` object of specifiable `indices` and `degree`, in addition to `entries`. A first non-tensor argument is assigned to the `entries`. Additional

TABLE II

TENSOR OBJECT CLASS DEFINITION. FAVOURING SIMPLICITY, THIS RELEASE OF THE `TENSOR` CLASS HAS A CONSTRUCTOR AND JUST THESE PUBLIC METHODS, INCLUDING OVERLOADED OPERATORS. ORDINARY METHODS ARE GROUPED TO FURTHER SIMPLIFY THE DISCUSSION.

Tensor Class (Value)
<p>Constructor, <i>etc.</i></p> <p><code>tensor (0, 1, 2+ args in)</code>, <code>index</code>, <code>entry</code>, <code>degree</code>, <code>ndims</code>, <code>numel</code>, <code>length</code>, <code>size</code>, <code>end ((,))</code></p> <p>Unary operations</p> <p><code>subsref ((,))</code>, <code>sum</code>, <code>permute</code>, <code>uminus (-)</code>, <code>uplus (+)</code>, <code>conj</code>, <code>not (~)</code>, <code>abs</code>, <code>log</code>, <code>round</code>, <code>transpose (.)'</code>, <code>ctranspose (')</code>, <code>trace</code>, <code>diag</code></p> <p>Binary operations</p> <p><code>subsasgn ((,)=)</code>, <code>plus (+)</code>, <code>minus (-)</code>, <code>eq (==)</code>, <code>ne (~=)</code>, <code>lt (<)</code>, <code>gt (>)</code>, <code>le (<=)</code>, <code>ge (>=)</code>, <code>and (&)</code>, <code>or ()</code>, <code>times (.*)</code>, <code>ldivide (.\)</code>, <code>rdivide (./)</code>, <code>power (.^)</code>, <code>mtimes (*)</code>, <code>mldivide (\)</code>, <code>mrdivide (/)</code></p> <p><i>N</i>-ary operations</p> <p><code>horzcat ([,])</code>, <code>vertcat ([;])</code>, <code>cat</code>, <code>isequal</code></p>

arguments must be `index` scalars or row vectors. The concatenated `index` arguments, extended if the result is too short compared to `ndims` minus two of the `entries`, is assigned to the `indices`. The `degree` exceeds `ndims` minus two when `index` arguments suffice to address trailing singleton (size one) dimensions of the `entries`.

Additional methods, `numel` and `length`, return the product of all dimension sizes and the size of the largest non-singleton dimension, respectively. They equal the `numel` and `length` of the `entries`. The `size` method invokes the `size` function, passing along parameters, on the `entries`. When all parameters are `index` objects, they convert first to numbers that represent MDA dimensions. The `end` method, needed for subscripting operations, `(,)` and `(,)=`, with numeric subscripts, requires `builtin` to invoke the `end` function on the `entries`, as `end` is also a keyword.

The RT software employs `index` objects with a logical NOT operator to represent contravariant indices as subscripts, alongside covariant ones. Whereas Table III suggests `index` subscripts are always required for nonzero-degree `tensor` expressions, the RT software enables a context-dependent `index`-free notation compatible with the RT algebra. For example, the inner product

TABLE III

TENSOR OBJECT UNIT TESTS. INCLUDED WITH THE RTTOOLBOX, THE `TENSOR` OBJECT UNIT TESTS ARE CHOSEN FOR THEIR TUTORIAL VALUE. TO ILLUSTRATE PROGRAMMATIC EFFICIENCY, SOFTWARE EXPRESSIONS ARE CROSS-REFERENCED TO EQUIVALENT ALGEBRAIC EXPRESSIONS. HERE, DN MEANS ANY-DEGREE AND D# MEANS DEGREE-#.

Algebraic expression (ref.)	Software expression
Inner product, D1 scalar (5)	<code>a(i)*b(i)*c(~i)</code>
Entrywise product, D1 scalar (7)	<code>a(i)*b(i)*c(i)</code>
Outer product, D1 scalar (9)	<code>a(i)*b(j)*c(k)</code>
Entrywise relation, D2 scalar (13)	<code>y(i,~j) ~ = y(~j,i)</code>
Permute and copy, D2 scalar (15)	<code>z(i,~j) = y(~j,i)</code>
Left division, D2 scalar (20)	<code>A(1,lp)\b(i,lp)</code>
Mixed product, D2 scalar (21)	<code>A(1,lp)*u(i,~l)</code>
Outer addition, D1 scalar (39)	<code>log(c(j)+x(i))</code>
Mixed product, D2 matrix (22)	<code>A(i,~j)*B(i,~j)</code>
Trace contraction, D2 matrix (25)	<code>trace(C(i,~i))</code>
Diagonal attraction, D2 matrix (27)	<code>diag(C(i,i))</code>
Inner product, DN vector (32)	<code>x(~k)'*x(~k)</code>
Col. concatenation, D1 vector (37)	<code>[ones(M,1) abs(c(i))]</code>
Row concatenation, D1 vector (37)	<code>[b(j).' ; ones(1,N)]</code>
Outer relation, D1 vector (38)	<code>A(i,~j) >= b(j).'</code>
Index concat., D2 matrix (40)	<code>cat(j,A(i,j),B(j,k))</code>

of an any-degree vector, `x`, with itself has a simpler form, `x'*x`, than the one shown. A `tensor` object always has `indices`, which may be specified or returned upon construction. Expressions that yield `tensor` results imply associated `indices` in predictable ways.

B. Index Objects

Table IV summarizes the constructor variants and methods, including overloaded operators, of the `index` class. Table V presents selected unit tests of class `index`. When a `tensor` object is constructed, its `indices` may be simultaneously dealt, as one or more `index` objects, to extra output arguments on the left-hand side (LHS) of an assignment.

A scalar `index` is constructed as follows. The object has two protected properties, `tilde`, itself an `index` object, and `state`, a logical variable. The `tilde` property of the `index` object's `tilde` property equals the `index` object itself. Moreover, the `state` of the `index` object and the `state` of its `tilde` property are always complementary. Upon construction,

TABLE IV

CLASS DEFINITION OF INDEX OBJECTS. ALTHOUGH THE CLASS HAS FEW OF ITS OWN METHODS, IT INHERITS PASS-BY-REFERENCE COPY AND (IN)EQUALITY OPERATORS FROM THE HANDLE CLASS. INHERITANCE ENABLES THE USE OF SET-THEORETIC FUNCTIONS (`ISMEMBER`, *etc.*) EXPLOITED BY THE TENSOR CLASS TO SUPPORT RICCI NOTATION.

Index Class (Handle)
Constructor, <i>etc.</i>
<code>index (0, 1 args in)</code> , <code>deal</code>
Unary methods
<code>logical</code> , <code>true</code> , <code>false</code> , <code>not (~)</code>

TABLE V

UNIT TESTS OF INDEX OBJECTS. EACH ENTRY OF AN INDEX OBJECT, WHICH MAY BE A VECTOR, EXPRESSES A TRUE (COVARIANT) OR FALSE (CONTRAVARIANT) CHARACTER. THESE TESTS ILLUSTRATE: (1) A SCALAR INDEX, (2) A VECTOR INDEX, (3) A ONE-STEP DEAL, (4) A WITH-TENSOR CONSTRUCTION, AND (5) A CAST-TO-LOGICAL.

```

%% Test1
k = index;
assert(isscalar(k))
assert(k ~ = ~k)
assert(k == ~~k)
assert(true(~k) == k)
assert(false(k) == ~k)
%% Test2
k = index(2);
[i, j] = deal(k);
assert(isscalar(i))
assert(isscalar(j))
assert(all(k == [i j]))
%% Test3
[i, j] = index(2);
assert(isscalar(i))
assert(isscalar(j))
%% Test4
sz = [100 100 10];
[A, k] = tensor(rand(sz));
assert(isa(k, 'index'))
%% Test5
k = [~index index(2)];
iscov = logical(k);
tf = [false true true];
assert(isequal(iscov, tf))

```

they are `true` and `false`, respectively. The constructor accomplishes this feat thanks in part to inheritance of the `handle` class and also via one-level recursion. A `handle` object resembles a `void` pointer in C/C++.

For a scalar index object, the `logical` method returns its `state` property (class `logical`) and the `true` or `false` methods return the index object itself or its `tilde` property (class `index`), whichever one has a `state` property equal to `logical true` or `false`, respectively. The NOT operator, overloaded by the `not` method, always returns the `tilde` property. In this fashion, the covariant, contravariant, or complementary index object is obtained, respectively.

As with the `logical` method, the `true`, `false`, and `not` methods work entrywise if the `index` object is nonscalar.

Because it inherits from class `handle`, class `index` does not need a `horzcat` method to enable `index` object concatenation into a row vector of class `index`. Kernel functions, like `length`, also work as expected. A variant of the `index` constructor accepts one argument, a number, to construct a row vector of class `index` with `length` equal to that number. The public `deal` method is invoked by the constructor to deal each entry of the row vector to output arguments in sequence. If there are fewer output arguments than the vector `length`, the last output argument is the vector remainder.

Upon construction, entries of an `index` object and their complements are unique, due to the `handle` superclass. Copy assignment, equality, and inequality operators are inherited. Entrywise equality of one `index` object to another, or to its complement via the entrywise NOT operator, offers a way to identify repeated indices, whether of the same character or not, in a `tensor` expression. Entrywise relational operators mean that set-theoretic functions like `ismember` and `unique`, which invoke a kernel `sort`, may be used with the `index` objects. As they are currently an interpreted part of the kernel, set-theoretic functions incur a reducible overhead.

Unlike the NT software, which uses template metaprogramming (LibNT), character vectors (NTToolbox), and counters (LibNT and NTToolbox) to represent indices of many possible characters, each `index` object of the RT software has only two possible characters. When used with the `tensor` class, `true` and `false` characters are called covariant and contravariant, respectively. In other contexts, `index` objects can represent one of two possible characters of any description.

C. Unary Operations

A `tensor` may be subscripted with `index`, numeric, or other objects on the right-hand side (RHS) or LHS of an (implied) assignment via overloaded `subsref` and `subsasgn` operators, respectively. Enclosing comma-separated subscripts in parentheses, the `subsref` operator is considered a unary operator on the `tensor` the parentheses follow. The `subsasgn` operator is considered a binary operator where one operand is the `tensor` the parentheses follow, on the LHS of the assignment, and the other operand is the result of an expression, on the RHS of the assignment.

When the `suboref` method is invoked, either all or none of the subscripts must be `index` objects. In the second case, the result of the `suboref` expression is an equivalent `suboref` expression applied to the `entries` of the `tensor`. The first case invokes a `simplify` method or throws an error. To avoid the runtime error, there must be at least as many indices, when subscripts are concatenated, as the `degree` of the `tensor`. Extra indices address trailing singleton dimensions of the `entries` and increase the `degree` of the `tensor` result. This feature supports a variety of outer operations.

The protected `simplify` method does two things. First, for each set of indices that match, irrespective of character, an attraction is performed. Second, for each set of attracted indices, a contraction is performed if at least one member is of a complementary character. Attracted indices that are not contracted have a unique character that are determined and assigned within the `indices` property of the returned `tensor`. All attractions are performed via one invocation of a protected method, `select`, that leverages kernel support for linear indexing. All contractions are performed via one invocation of an overloaded and public `sum` method.

After converting `index` arguments to numeric dimensions, the `sum` method invokes a kernel `sum` on the `entries` of a `tensor`, passing on arguments. A kernel `ismember` tests membership of concatenated `index` arguments in the `indices`, finding dimensions of `entries`. With the `true` method, the `index` test is done irrespective of character. Before invoking `sum` on the `entries`, dimensions from matched `indices` are increased by two, as first and second dimensions address rows and columns of `entries`, respectively. Unmatched `index` arguments address trailing singleton dimensions, which always exist, of the `entries`.

Though the `subsasgn` operator is binary, it relies on the unary `permute` method. The latter requires either all-`index` or all-numeric arguments. Before invoking a kernel `permute` on the `entries` property, passing along all arguments, the `index` arguments find equivalent numeric dimensions. The `permute` method updates the sequence of returned indices, which make up the `indices` property, to correspond.

In the case where all (other) arguments are `index` objects, when the `permute` method is invoked on a `tensor` object, a comparison is made between the `indices` property, the old indices, and the `index` arguments, the new indices. All old indices must be retained, character unchanged. Additional new indices, which find trailing singleton dimensions, are allowed, in which case the `degree` increases. Each new `index` of a permuted `tensor` has the character as specified.

Unlike `subsasgn`, `subsref` never invokes `permute`. A `subsref` operation with index subscripts ignores preexisting indices of the tensor operand. Concatenated index subscripts simply redefine indices of the returned tensor, notwithstanding contractions and attractions, which eliminate indices, reduce degree, and modify entries.

The remaining unary methods of class `tensor`, operators included, may be divided into entrywise and pagewise groups. Entrywise unary methods, from `uminus` to `round`, apply a corresponding kernel function to the `entries` property. The `round` method, allowing a precision argument, illustrates a parameterized operation. Parameters are passed unchanged to the kernel function applied to the `entries` property.

Two pagewise methods, `transpose` and `ctranspose`, invoke kernel `pagetranspose` and `pagectranspose` functions on the entries of a tensor. These functions are like a for loop over third and additional dimensions of the MDA where to each page, a contiguous 2D array of the first two dimensions, a kernel `transpose` or `ctranspose` is applied. Two other kernel functions for 2D arrays, `trace` and `diag`, were likewise extended for MDAs into `pagetrace` and `pagediag` functions. They are invoked on entries of a tensor by pagewise `trace` and `diag` methods.

D. N-ary Operations

Kernel `horzcat` and `vertcat` functions compute column and row concatenations, respectively, for MDAs. These familiar N -ary operations, for vectors, matrices, and arrays of compatible dimensions, when overloaded by the `tensor` class as `horzcat` and `vertcat` methods, involve N operands at once. Each overloaded method invokes a protected `alignn` method to modify each operand into a suitable MDA prior to a `pagehorzcat` or `pagevertcat` invocation that produces the entries of the initial result tensor. The `alignn` method also supplies the indices of the initial result. The final result tensor is produced after contractions, specified by `alignn`, are computed using the `sum` method.

The `alignn` method inputs N and outputs $N + 2$ arguments. For each tensor input only its entries, an MDA, is output. Via a kernel `permute`, the MDA is modified so that its dimensions align based on the set-theoretic union, in sequence, of indices irrespective of character. A non-tensor input passes to an output only if it is a 2D array. One additional output is the set-theoretic union of indices, character and left-to-right sequence preserved.

If both characters appear the leftmost one is chosen. The second additional output, an `index` vector, specifies which indices require contraction, i.e., ones where both characters appeared.

To support outer concatenation, possible at non-row/column dimensions, `pagehorzcat` and `pagevertcat` invoke `pagecat` on the N (permuted) MDAs from the `alignn` method. Corresponding non-singleton dimensions must equate in size except for the dimension at which concatenation is performed. As kernel `horzcat`, `vertcat`, and `cat` do not support outer concatenation, singleton dimensions in the third or higher position are expanded, using one kernel `repmat` per operand, to match expected sizes of corresponding dimensions after concatenation, now performable via a kernel `cat`.

Generalizing concatenation further, the `cat` method implements `index` concatenation. In its `InferiorClasses` list, the `tensor` class includes the `index` class so that the former's `cat` method is invoked in a `cat` expression where the first argument is an `index` object. The `cat` method converts the first argument, as required, into a number that specifies the dimension of concatenation, considering the `alignn` step. Apart from invoking `pagecat` directly, passing along the dimension of concatenation, the `cat` method is thereafter identical to the `horzcat` and `vertcat` methods.

The `isequal` and `round` methods help verify unit tests. Implementation of `isequal` is similar to `horzcat` and `vertcat`. However, the `isequal` method instead of a `tensor` returns a `logical`, equal to the result of a kernel `isequal`, also N -ary, invoked instead of `pagehorzcat` or `pagevertcat` on the MDAs from `alignn`. Moreover, instead of contractions the `isequal` method always returns `false` if one operand has an `index` of one character and another operand has the same of the complementary character. This result is congruous with how the kernel `isequal` of a column vector and its `transpose`, a row vector having identical entries in the same sequence, returns `false`.

In theory, MATLAB could invoke a single overloaded method for an N -ary product expression involving a `tensor`. However, it invokes a sequence of binary product methods with a left-to-right precedence rule. Prior to RT software expression, this rule may require modification of an RT algebraic expression. In particular, to express an N -ary inner product over an `index` all but the rightmost operand must have the same character, covariant or contravariant, for that `index`, with only the rightmost operand having a complement.

The NT software has two deviations from its NT algebra. To correctly compute some expressions, one or more sub-expressions have to be enclosed in parentheses and preceded by an extra

operator, whose purpose is to decrement internal counters associated with underline-equivalent operators on enclosed indices. For this purpose, the tilde operator is hijacked. Thus, it cannot represent the entrywise NOT of a `DenseNT`, a tensor class of the `NTToolbox`. These deviations represent additional weaknesses, this time from a constructivism angle, of NT underline and multi-index notation formalisms.

E. Binary Operations

When the `subsasgn` method is invoked, for a `tensor` operand on the LHS of an assignment, it provides parameters, namely subscripts of the LHS operand, in addition to the RHS operand. If all subscripts are `index` objects the assignment overwrites the LHS operand with the RHS one after its `permute` method is invoked so that `indices` are in the sequence specified by the LHS subscripts and not the RHS operand, required to be a `tensor`. If the RHS operand is not a `tensor` here, a runtime error results. If all LHS subscripts are numbers, the kernel's `subsasgn` function is applied to the LHS `entries` with those subscripts and either the original RHS operand, if not a `tensor`, or its `entries`.

Entrywise binary methods, from `plus` to `power` in Table II, each invoke a protected method, `binary`, passing operands along as second and third arguments. The first argument is a handle, e.g., `@plus`, to an entrywise kernel function. Within `binary`, after it invokes a protected `alignn` on the operands, there are two `index` vectors and two MDAs. To compute initial `entries` of the final `tensor`, the entrywise kernel function is applied to the aligned MDAs. With the first `index` vector from `alignn` as initial `indices`, an initial `tensor` is produced using the two-argument constructor. Using the second `index` vector to specify contractions, the `sum` method is invoked to produce the final `tensor`.

Remaining binary methods, `mtimes`, `mldivide`, and `mrdivide`, are called *pagewise* because they exploit kernel `pagemtimes`, `pagemldivide`, and `pagemrdivide` functions through protected methods, namely `mbinary`, `mbinary2`, `align2`, and `pageify`. Each *pagewise* binary method invokes the `mbinary` method with a kernel function handle, e.g., `@pagemtimes`, as the first argument. For computational efficiency, the design involves a minimal number of kernel `reshape` and `kernel permute` invocations.

The *pagewise* binary methods exploit the *lattice* concept. A lattice is a degree-one matrix represented as a 3D array. The matrix may be vector or scalar, depending on dimension sizes, and there may be one page. Lattices help to realize an arbitrary inner, outer, and entrywise

times between two tensor operands. Each operand maps (permute-and-reshape) to a lattice, \mathbf{A} or \mathbf{B} , a lattice product executes as follows, and the result lattice, \mathbf{C} , maps (reshape-and-permute) to a tensor with indices as required by the RT algebra:

$$\mathbf{C}_k = \mathbf{A}_k \mathbf{B}_k. \quad (98)$$

All outer products are represented by rows of the first lattice, \mathbf{A} , and columns of the second lattice, \mathbf{B} . All inner products are represented by columns and rows, respectively, of the first and second lattices. The common page dimension represents all entrywise products, which may execute in parallel.

Similarly, the RT software implements `mldivide` and `mrdivide` consistent with the RT algebra. Such left- or right-divisions imply a solution to a corresponding linear system, allowing inner, outer, and entrywise products. These map to and from a left- or right-division of lattices, as follows:

$$\mathbf{B}_k = \mathbf{A}^k \setminus \mathbf{C}_k, \quad (99)$$

$$\mathbf{A}_k = \mathbf{C}_k / \mathbf{B}^k. \quad (100)$$

As with division of scalars, indices of denominator operands have to change character. Otherwise, the RT framework would be inconsistent in the context of linear systems. Prior to invoking `mbinary`, the `mldivide` and `mrdivide` methods complement indices using the `not` method.

The `mbinary` method receives the operands of a pagewise binary method as second and third arguments. If either operand is not a tensor then it must be a 2D array to avoid a runtime error by design. With a 2D array operand the tensor result has the same indices as the tensor operand. Resulting entries equal the result of a pagewise function, specified via a handle, applied to the tensor operand's entries and the non-tensor operand. Because linear system operations are non-commutative, in general, pagewise function operands follow the original sequence received by `mbinary`.

When both operands of `mbinary` are tensor objects, the method invokes `mbinary2` on them. After `mbinary2` returns, `mbinary` has from it the final indices of the operation, two MDAs, and two vectors that specify a kernel `reshape-and-permute`. To compute the final entries of the original operation, `mbinary` applies a pagewise function, specified via a handle, to the two MDAs, in the order received, followed by the kernel `reshape-and-permute`.

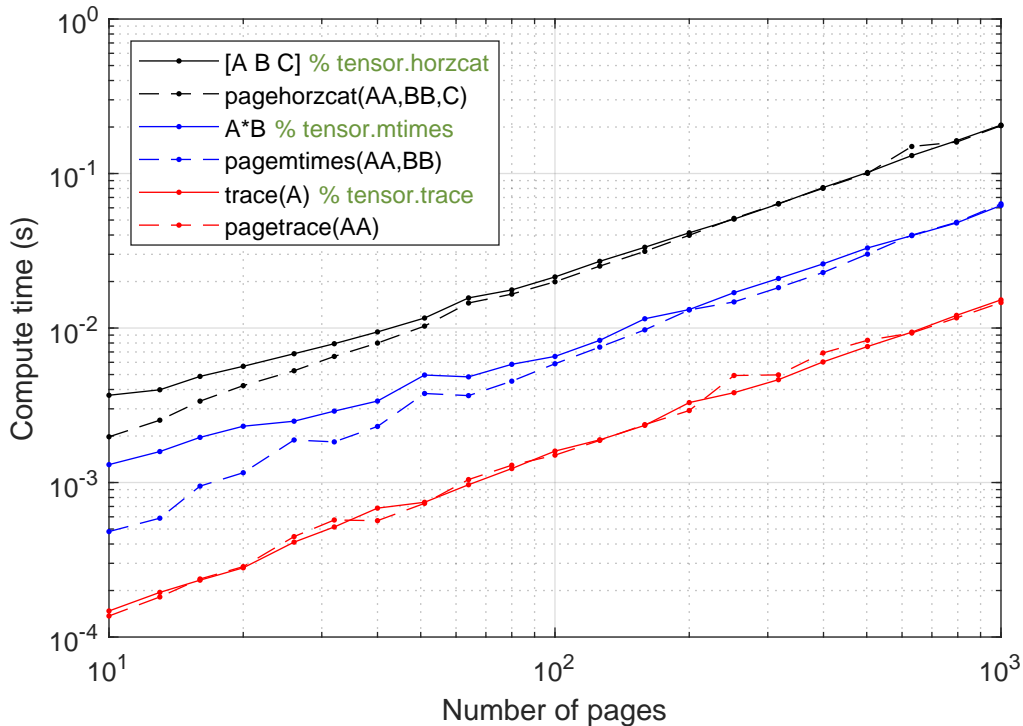


Fig. 5. Abstraction penalties vs. dimension size. The interpreted RTToolbox is computationally efficient when underlying unary, binary, or ternary operations involve large enough operands. In these tests, `tensor` operands have the same dimension sizes, $100 \times 100 \times P$. Tests vary a page dimension size, P .

The `mbinary2` method invokes an `align2` method that depends only on indices of each operand. This results in matching and leftover indices for each operand. Additional vectors indicate whether matching indices have the same character. After `align2` is done, `mbinary2` knows which dimensions of each operand's entries correspond in inner, entrywise, and outer fashion. Using this information, a kernel `permute-and-reshape` is applied separately, via the `pageify` method, to each operand's entries. Along with resulting MDAs, the `mbinary2` method returns information to `mbinary` for its kernel `reshape-and-permute`.

Figure 5 presents representative abstraction penalties of RT software, when operands are small enough, and computational efficiencies, when operands are large enough. In examples of unary, binary, and ternary operations with compatible dimension sizes, two operands, `A` and `B`, are degree-one matrices each constructed as a `tensor` with the same scalar index. Other operands, `C` or `AA` and `BB`, are 2D or 3D arrays.

For the Figure 5 results, each operand or its entries is an array of class `double` with `rand`

values. Compute times are averaged over multiple runs. Results are compared for equivalent operations done without `tensor` and `index` classes. In the binary case, the equivalent computation uses a kernel `pagewise` function. Although a kernel `mtimes`, for 2D arrays, may be applied to MDAs in `pagewise` fashion with one or more `for` loops (interpreted), the kernel `pagemtimes` (compiled) does the same but faster. As no kernel `pagewise` functions (interpreted or compiled) exist for the unary and N -ary cases, the comparisons use RTToolbox functions (interpreted).

The RT software expresses the RT algebra with programmatic efficiency. When abstraction penalties are small, relative to equivalent computations requiring only the kernel and novel `pagewise` functions, the RT software achieves computational efficiency. Currently, kernel set-theoretic functions are interpreted not compiled. As they are critical to the RT abstraction, they are a key source of penalties. So that the RTToolbox obeys toolbox requirements of the MATLAB Central File Exchange, it was designed without compilable MEX files, such as C/C++ implementations of kernel set-theoretic functions.

V. CONCLUSIONS

This paper introduced an RT framework, the successor to a published NT framework, both of which complement a popular EMV framework. Comprising an underlying RT algebra and associated RT software, to model a problem and trial a solution thereof, the proposed RT framework represents an alternative for model-based imaging approaches involving tensors.

The RT algebra inherits advantages of the NT algebra, with respect to N -degree support, associativity, commutativity, entrywise products, linear invertibility, and other previously published considerations. However, due to its extended dual-index notation, as opposed to the *de facto* multi-index notation of the NT algebra, the RT algebra provides all the expressivity of the NT algebra in a simpler way. Thanks to additional outer operations, inspired by EMV broadcasting, the RT algebra is also more expressive than the NT one. As it aligns better with the Ricci notation of non-Euclidean geometry, the RT algebra lays a foundation for tensor approaches beyond numeric.

Relevance of the RT algebra to model-based imaging is illustrated with a tutorial example. The example demonstrates an asymptotically-efficient solution of an optimization problem where the SSE, a scalar function of deviant pixels in the image plane, depends on an unknown phase offset in the pupil plane, a 2D Fourier domain. The RT algebra helps to model and simplify the SSE and its first and second derivatives, namely a gradient and an HMF, where the complexity

of computing all three proves equivalent to computing just the SSE only. The approach makes visible diffraction rings and exoplanets near an occulted star in a simulated coronagraph image.

Thanks to the RT algebra, all nonzero-degree matrices in the gradient expression were eliminated. Moreover, gradient and HMF expressions were reorganized to reveal embedded 2D (inverse) DFTs, acceleratable via 2D (inverse) FFTs. Whereas the asymptotic time-and-space efficiencies of the tutorial example were realizable without the RT software, using it helped. A natural implementation of the RT algebra simplified a validation of intermediate steps in the underlying derivation. During the search for asymptotic efficiencies, algebraic errors were corrected via concurrent RT software sanity checks.

The RT software is defined as the RTToolbox, comprising `tensor` and `index` classes, new pagewise functions, and unit tests, plus MATLAB. In this manner, the RT framework complements a popular EMV framework. Methods, functions, and tests presented, a subset of what could be developed, are chosen to emphasize key software requirements. Arguing that additional computational efficiency is possible, the approach taken emphasizes programmatic efficiency. Allowing the RT algebra to be naturally expressed with MATLAB, the RTToolbox is designed in a way where small abstraction penalties, related to `index` objects, would reduce with a MATLAB release that compiled kernel set-theoretic functions.

Compared to the NT software for MATLAB end users, comprising a C/C++ library called LibNT, M-file and MEX wrappers of the NTToolbox, plus MATLAB itself, the RT software is simpler, comprising only M-files of the RTToolbox plus MATLAB. Although the NTToolbox has a tensor class called `DenseNT`, it relies on MATLAB character vectors and string processing to represent indices and parse its multi-index notation. Not only does the RTToolbox use an object-oriented approach to support its dual-index notation, but it inherits the kernel `handle` class (congruous to C/C++ `void` pointers) for added programmatic and computational efficiency.

Finally, the paper elaborated on codesigned unary, binary, and N -ary operations, e.g., to express an N -ary inner product, the RT software may vary from the RT algebra. As MATLAB parses an N -ary product into a binary product sequence with left-to-right precedence, all but the rightmost one must be entrywise to express an N -ary inner product over an index. This variation is contrasted with those of the NT software, which unlike the NT algebra required some products to be enclosed in parentheses and preceded with an additional operator. Other than introducing a left-to-right precedence rule, the RT software expresses the RT algebra faithfully.

ACKNOWLEDGMENTS

The author gratefully acknowledges editorial advice from Adam P. Harrison, whose NT framework laid a foundation for this work, and Dan Sirbu, who suggested motivating the RT framework with a model-based example involving DFTs.

REFERENCES

- [1] M. Abadi, P. Barham, J. Chen, *et al.*, “TensorFlow: A system for large-scale machine learning,” *arXiv:1605.08695v2 [cs.DC]*, 1–18 (2016).
- [2] N. Vasilache, O. Zinenko, T. Theodoridis, *et al.*, “Tensor Comprehensions: Framework-Agnostic High-Performance Machine Learning Abstractions,” *arXiv:1802.04730v3 [cs.PL]*, 1–37 (2018).
- [3] T. Mai, E. Lam, and C. Lee, “Deep Unrolled Low-Rank Tensor Completion for High Dynamic Range Imaging,” *IEEE Transactions on Image Processing* **31**, 5774–5787 (2022).
- [4] P. Wang, T. Cao, X. Li, *et al.*, “Multi-focus image fusion based on gradient tensor HOSVD,” *Journal of Electronic Imaging* **32**(2), 023028 1–18 (2023).
- [5] C. Prévost, R. Borsoi, K. Usevich, *et al.*, “Hyperspectral Super-resolution Accounting for Spectral Variability: Coupled Tensor LL1-Based Recovery and Blind Unmixing of the Unknown Super-resolution Image,” *SIAM Journal on Imaging Sciences* **15**(1), 110–138 (2022).
- [6] X. Liu, C. Hao, Z. Su, *et al.*, “Image inpainting by low-rank tensor decomposition and multidirectional search,” *Journal of Electronic Imaging* **30**(5), 053010 1–21 (2021).
- [7] J. Bengua, H. Phien, H. Tuan, *et al.*, “Efficient Tensor Completion for Color Image and Video Recovery: Low-Rank Tensor Train,” *IEEE Transactions on Image Processing* **26**(5), 2466–2479 (2017).
- [8] E. Newman and M. Kilmer, “Nonnegative Tensor Patch Dictionary Approaches for Image Compression and Deblurring Applications,” *SIAM Journal on Imaging Sciences* **13**(3), 1084–1112 (2020).
- [9] S. Lefkimmatis and S. Osher, “Nonlocal Structure Tensor Functionals for Image Regularization,” *IEEE Transactions on Computational Imaging* **1**(1), 16–29 (2015).
- [10] M. Rezaghi, “A Novel Fast Tensor-Based Preconditioner for Image Restoration,” *IEEE Transactions on Image Processing* **26**(9), 4499–4508 (2017).
- [11] M. Marquez, H. Rueda-Chacon, and H. Arguello, “Compressive Spectral Light Field Image Reconstruction via Online Tensor Representation,” *IEEE Transactions on Image Processing* **29**, 3558–3568 (2020).
- [12] W. Qiu, J. Zhou, and Q. Fu, “Tensor Representation for Three-Dimensional Radar Target Imaging With Sparsely Sampled Data,” *IEEE Transactions on Computational Imaging* **6**, 263–275 (2020).
- [13] Y. Li, J. Zhang, G. Sun, *et al.*, “Hyperspectral image compressive reconstruction with low-rank tensor constraint,” *Journal of Electronic Imaging* **29**(2), 023009 1–13 (2020).
- [14] H. Skibbe and M. Reisert, “Spherical Tensor Algebra: A Toolkit for 3D Image Processing,” *Journal of Mathematical Imaging and Vision* **58**(3), 349–381 (2017).
- [15] W. Zhou, L. Shi, Z. Chen, *et al.*, “Tensor Oriented No-Reference Light Field Image Quality Assessment,” *IEEE Transactions on Image Processing* **29**, 4070–4084 (2020).
- [16] E. Solomonik, D. Matthews, J. Hammond, *et al.*, “A massively parallel tensor contraction framework for coupled-cluster computations,” *Journal of Parallel and Distributed Computing* **74**(12), 3176–3190 (2014).

- [17] N. Singh, Z. Zhang, X. Wu, *et al.*, “Distributed-memory tensor completion for generalized loss functions in python using new sparse tensor kernels,” *Journal of Parallel and Distributed Computing* **169**, 269–285 (2022).
- [18] M. Valiev, E. Bylaska, N. Govind, *et al.*, “NWChem: A comprehensive and scalable open-source solution for large scale molecular simulations,” *Computer Physics Communications* **181**(9), 1477–1489 (2010).
- [19] K. Kowalski, R. Bair, N. Bauman, *et al.*, “From NWChem to NWChemEx: Evolving with the Computational Chemistry Landscape,” *Chemical Reviews* **121**(8), 4962–4998 (2021).
- [20] G. Baumgartner, A. Auer, D. Bernholdt, *et al.*, “Synthesis of High-Performance Parallel Programs for a Class of *Ab Initio* Quantum Chemistry Models,” *Proceedings of the IEEE* **93**(2), 276–292 (2005).
- [21] E. Mutlu, A. Panyala, N. Gawande, *et al.*, “TAMM: Tensor Algebra for Many-body Methods,” *arXiv:2201.01257v3 [cs.DC]*, 1–13 (2023).
- [22] J. Kossaifi, Y. Panagakis, A. Anandkumar, *et al.*, “TensorLy: Tensor Learning in Python,” *Journal of Machine Learning Research* **20**, 925–930 (2019).
- [23] Y. Panagakis, J. Kossaifi, G. Chrysos, *et al.*, “Tensor Methods in Computer Vision and Deep Learning,” *Proceedings of the IEEE* **109**(5), 863–890 (2021).
- [24] P. Cumpson, N. Sano, I. Fletcher, *et al.*, “Multivariate analysis of extremely large ToFSIMS imaging datasets by a rapid PCA method,” *Surface and Interface Analysis* **47**(10), 986–993 (2015).
- [25] C. Bedia, A. Sierra, and R. Tauler, “Application of chemometric methods to the analysis of multimodal chemical images of biological tissues,” *Analytical and Bioanalytical Chemistry* **412**, 5179–5190 (2020).
- [26] A. Harrison and D. Joseph, “Numeric tensor framework: Exploiting and extending Einstein notation,” *Journal of Computational Science* **16**, 128–139 (2016).
- [27] B. Bader and T. Kolda, “Algorithm 862: MATLAB Tensor Classes for Fast Algorithm Prototyping,” *ACM Transactions on Mathematical Software* **32**(4), 635–653 (2006).
- [28] T. Kolda and B. Bader, “Tensor Decompositions and Applications,” *SIAM Review* **51**(3), 455–500 (2009).
- [29] L. Sorber, M. Van Barel, and L. De Lathauwer, “Structured Data Fusion,” *IEEE Journal of Selected Topics in Signal Processing* **9**(4), 586–600 (2015).
- [30] N. Vervliet, O. Debals, L. Sorber, *et al.*, “Breaking the Curse of Dimensionality Using Decompositions of Incomplete Tensors: Tensor-based scientific computing in big data analysis,” *IEEE Signal Processing Magazine* **31**(5), 71–79 (2014).
- [31] I. Oseledets, “Tensor-Train Decomposition,” *SIAM Journal on Scientific Computing* **33**(5), 2295–2317 (2011).
- [32] J. Synge and A. Schild, *Tensor Calculus*, Dover Publications (1978).
- [33] The MathWorks, “Create and Share Toolboxes.” MATLAB R2022a Documentation (2022).
- [34] The MathWorks, “Page-wise matrix multiplication (`pagemtimes`).” MATLAB R2020b Documentation (2020).
- [35] D. Sirbu, N. Kasdin, and R. Vanderbei, “Monochromatic verification of high-contrast imaging with an occulter,” *Optics Express* **21**(26), 32234–32253 (2013).
- [36] D. Sirbu, S. Thomas, R. Belikov, *et al.*, “Demonstration of broadband contrast at $1.2 \lambda/D$ and greater for the EXCEDE starlight suppression system,” *Journal of Astronomical Telescopes, Instruments, and Systems* **2**(2), 025002 1–14 (2016).
- [37] D. Sirbu, S. Thomas, R. Belikov, *et al.*, “Techniques for High-contrast Imaging in Multi-star Systems. II. Multi-star Wavefront Control,” *The Astrophysical Journal* **849**(2), 1–13 (2017).
- [38] W. Schulz, “Digging the Dark Hole: Coronagraphy and the Quest to Find Other Worlds,” *Photonics Focus* **4**(3), 22–27 (2023).
- [39] Wikipedia contributors, “Airy disk — Wikipedia, The Free Encyclopedia.” https://en.wikipedia.org/w/index.php?title=Airy_disk (2022). [Online; accessed 21-July-2022].